A global analysis of wave potential energy in the lower stratosphere derived from 5 years of GPS radio occultation data with CHAMP

A. de la Torre,[1] T. Schmidt,[2] and J. Wickert[2]

Received 28 July 2006; revised 9 October 2006; accepted 18 October 2006; published 20 December 2006.

[1] This paper presents the first results of the global long-term potential energy and mean potential energy per unit mass associated to wave activity (WA) in the lower and middle stratosphere, obtained from Global Positioning System radio occultation (GPS-RO) temperature profiles, retrieved during the last 5 years from the CHAMP (CHAllenging Minisatellite Payload) satellite. We excluded temperature variations corresponding to the wavelike character of the Quasi Biennial oscillation (QBO). Possible limitations and distortions expected from our analysis are pointed out. Systematic annual and interannual features, clearly evidenced through 5 years of observations as a function of height, latitude and time are shown. We confirm some previously reported characteristics, in particular interannual requiring a sufficiently long period of observation, in addition to others not reported yet. In particular, a general stronger (weaker) wave activity is observed associated to apparent vertical wavelengths longer (shorter) than 4 km. The tropical/extratropical signatures decrease/increase with increasing altitude. At equatorial latitudes, WA interannual enhancements, related to QBO, are observed just below zonal wind zero contours corresponding to westerly shears. A significant decrease of WA is seen where the zonal wind is minimum. Both at equatorial and middle latitudes, an increased WA appears close above the TP, following its annual height oscillation and above 30 km height. At higher latitudes, a systematic annual variation of WA is observed, exhibiting stronger enhancements in winter SH respect to NH, but in SH, taking place during late winter and early spring. This enhanced WA, associated during 2002 to the stratospheric warming observed in that year, appears here as a systematic annual stratospheric feature. Its intensity increases with altitude, from 25 to 35 km. Inertio-gravity waves generated by geostrophic adjustment during the maximum of the southern polar vortex (polar night jet) between late August and mid- September, could constitute a main source of this WA enhancement. **Citation:** de la Torre, A., T. Schmidt, and J. Wickert (2006), A global analysis of wave potential energy in the lower stratosphere derived from 5 years of GPS radio occultation data with CHAMP, *Geophys. Res. Lett.*, *33*, L24809, doi:10.1029/2006GL027696.

1. Introduction

[2] In the last years, several analyses based on radiosonde and satellite data on global energy distribution associated to atmospheric waves in the lower stratosphere were performed [see, e.g., *Fritts and Alexander*, 2003]. Nevertheless, as *Alexander* [1998] pointed out, no observational technique is able by itself to contemplate the whole spectrum of gravity waves (GWs). The radio occultation (RO) measurement principle was applied in various studies to observe the Earth's atmosphere and climate [see, e.g., *Wickert et al.*, 2005]. Since 2001, from the German Low Earth Orbit (LEO) satellite CHAMP (CHAllenging Minisatellite Payload), atmospheric parameters such as temperature, pressure, water vapor and geopotential height have been obtained. Simultaneous global coverage, sub-Kelvin temperature accuracy, high vertical resolution and insensitivity to clouds make this technique unique. Climatologies from global observations during long-term periods are essential to understand the role that GWs play in atmosphere circulation. *Tsuda et al.* [2000], from a RO data set obtained during the GPS/MET (Global Positioning System/Meteorology) experiment from April 1995 to February 1997, evaluated the global wave potential energy in the stratosphere as a function of latitude, longitude and height, obtaining enhanced values around the Equator with considerable longitude variations, and at higher latitudes, in the winter hemisphere. *Venkat Ratnam et al.* [2004] performed a global study of GW activity in the stratosphere from CHAMP RO data retrieved from May 2001 to January 2003. They found large potential energy values at tropical latitudes and at midlatitudes during winter, larger over continents than over oceans in both hemispheres, but during equinoxes, only larger at tropical latitudes. They found large(low) values of potential energy below(above) 25 km altitude during all seasons in the tropics (30°N–30°S), increasing again above 30 km. Large values were observed during the stratospheric warming of September 2002. *Randel and Wu* [2005] studied the Kelvin wave variability from GPS-RO data gathered along two years, observing enhanced amplitudes coincident with the descending westerly shear phase of the QBO. In this paper we present the first results of the WA global distribution in the lower stratosphere, from a long-term GPS-RO data set (5 years, from May 2001 to April 2006). The long interval considered allowed to confirm the significance of annual and interannual WA features previously reported, as well as the identification of new ones. Some features are related to the Quasi Biennial oscillation (QBO) nevertheless, we excluded the QBO temperature variability itself. Possible observational limitations and distortions expected from any GPS-RO wave analysis are pointed out.

2. The Specific Potential Wave Energy

[3] The mean specific (per unit mass) potential energy associated with a single monochromatic wave of vertical

[1]Departamento de Física, Facultad de Ciencias Exactas y Naturales, Universidad de Buenos Aires, Buenos Aires, Argentina.
[2]Geodesy and Remote Sensing, GeoForschungsZentrum Potsdam, Potsdam, Germany.

0094-8276/06/2006GL027696

length λ_z, $E_{P\lambda_z}$, represents a measure of its total wave energy [see, e.g., *Gill*, 1982], and involves an integral over a vertical column equal to one wavelength: $E_{P\lambda_z} = \lambda_z^{-1} \int_0^{\lambda_z} E_P dz$, where $E_P = g^2\delta T^2/2N^2T_B^2$ is the specific potential energy, and g, N, δT, T_B and z are, respectively, the acceleration of gravity, the buoyancy frequency, the band-pass filtered temperature perturbation, the background temperature and the altitude. Any difference between the chosen limits of integration not equal to a multiple of one wavelength will modify $E_{P\lambda_z}$. A similar consequence will affect an ensemble of waves. Assuming a statistical balance between the excess and defect phase contributions of each wave in the ensemble, a fixed vertical column C of a few kilometers may be considered to integrate E_P, thus yielding E_{PC}. GPS-RO T observations represent an ''observational filter'' [*Alexander*, 1998] that includes an ensemble of gravity, inertio-gravity and planetary waves, with λ_z less than about 10 km. As *Wu et al.* [2006] pointed out, the sensitivity upper limit of GPS-RO measurements, caused by the detrending, is consistent with our choice, as we only analyze λ_z with an upper cutoff at 10 km. Vertical filtering is applied here. We do not intend to distinguish among energy contributions belonging to each source of GWs (orographic forcing, deep convection, geostrophic adjustment and shear instabilities [see, e.g., *Fritts and Alexander*, 2003]) and to planetary waves. During any wave analysis based on GPS-RO data, the observational filter and consequently the calculated E_P, may be affected in different ways: i) A part of the wave spectrum is rejected by filtering out scales longer than 10 km; ii) a discrepancy is expected between ''actual'' and ''apparent'' λ_z, due to the non-vertical line of sight (LOS) followed during the atmospheric soundings [*de la Torre and Alexander*, 1995], in a scenario of phase surfaces distributed over a wide range of wave propagation bending angles; iii) the wavelength refraction in a ground-fixed frame of reference imposed by a variable background mean wind [*Alexander*, 1998] and iv) the uncertain capability of RO measurements to detect short horizontal wavelengths, considering the relative direction between LOS and GW successive phase surfaces [*de la Torre and Alexander*, 2005]. All these distortions may derive in possible over(under)estimations of E_P and consequently, of E_{PC}.

3. Description of Observed WA Structures

[4] The spatial and temporal structure of the observed WA variability, is presented below as a function of latitude, z and time. Here, longitudinal variability is not discussed. We subdivided both hemispheres in independent, adjacent cells of 10° per 10° in longitude and latitude respectively. The retrieved $T(z)$ profiles, previously processed, were splined with a 200 m step (larger steps did not essentially alter the resulting profiles). The band-passed T fluctuations, δT, between cut-offs z_1 and z_2 ($z_1 < z_2$), were calculated as follows. The T profiles were first low pass filtered, with a cut-off at z_2, obtaining T_B. The filter was applied again to the difference $T - T_B$, now with a cut-off at z_1, thus yielding δT, which isolates wavelengths between z_1 and z_2. Two different non-recursive filters were tested [*Scavuzzo et al.*, 1998; *Schönwiese*, 2000], with almost identical results. A Kaiser window was used to avoid Gibbs effects. In Figure 1a, we show the latitude-month distribution of E_{PC} in the stratosphere, between 1 km above the TP (see explanation below) and 35 km height. Dashed vertical lines indicate the beginning of each year. After testing possible artifacts close to the TP caused by the filtering process, we observed that these essentially lie in a z interval within ±1 km.

[5] The successful reproduction of the TP T minimum from GPS-RO data is well known nevertheless, we are still testing alternative methods to minimize artificial WA enhancements there. The detailed WA description at the TP/s will be discussed elsewhere. The subdivision in adjacent and non-overlapping cells of 10° of latitude and one month, allows for a better geographic identification of WA distribution, avoiding the contamination of energy exhibited in a wide and diffuse region around each cell. In Figure 1, the space-time structures correspond to waves of different origin. From previous observational and theoretical studies [see, e.g., *Vincent and Alexander*, 2000, *Tsuda et al.*, 2000] we know that these waves correspond to a complex ensemble built up from diverse sources. Besides the expected accumulation of wave energy around the Equator, the identification and localization of wave sources clearly represents a challenge by itself. A concentration of WA between 10°N and 10°S, with maximum around 7 J/kg decreasing towards 30°N/S is observed. If an annual or interannual variability exists, as it is the case -see below-, it is not still clear here. At higher latitudes, a systematic annual variation of WA is observed during the five years analyzed, exhibiting defined enhancements in winter Hemisphere. This feature has been already pointed out by several authors [see, e.g., *Venkat Ratnam et al.*, 2004]. Nevertheless, in winter SH the annual enhancements seem to be i) more intense and ii) taking place during late winter and early spring. The systematic delay in high latitude SH maximums with respect to winter (June-July), not observed in NH, are clear here from a 5-year observation period. *Yoshiki and Sato* [2000], from polar radiosoundings launched during a 10-year period, reported an enhanced WA at high latitudes likely related to the polar night jet. In Figure 1, we are integrating WA in vertical columns always higher than 15 km. This conceals a strong non-uniform stratification of WA in the stratosphere. To enhance our understanding of the origin and spatial distribution of these features, two approaches were introduced: In Figures 1b and 1c, in order to get a better insight into the relative significance of the expected different sources of GWs, before calculating E_P, we make a separation into longer (4–10 km) and shorter (<4 km) λ_z. This separation is obviously still affected by the observational constraints discussed in section 2, last paragraph, but provides a useful first approach to a comprehensive understanding of the problem [*de la Torre et al.*, 2004]. In Figure 1b, E_{PC} maximum values near 4 J/kg are frequent, roughly 2 times the maximum registered in 1c. Clear enhancements around the Equator are identified at the end and beginning of 2002, 2004 and 2006. This interannual feature is not seen in Figure 1c, and is related, through different mechanisms, to QBO (see below) [*Randel and Wu*, 2005]. In Figure 1b, the annual five enhancements observed at high latitudes in SH and NH, and the time drift towards the Southern Spring Equinox mentioned above, are more clear than in Figure 1a. For shorter λ_z (Figure 1c), these effects appear more diffuse.

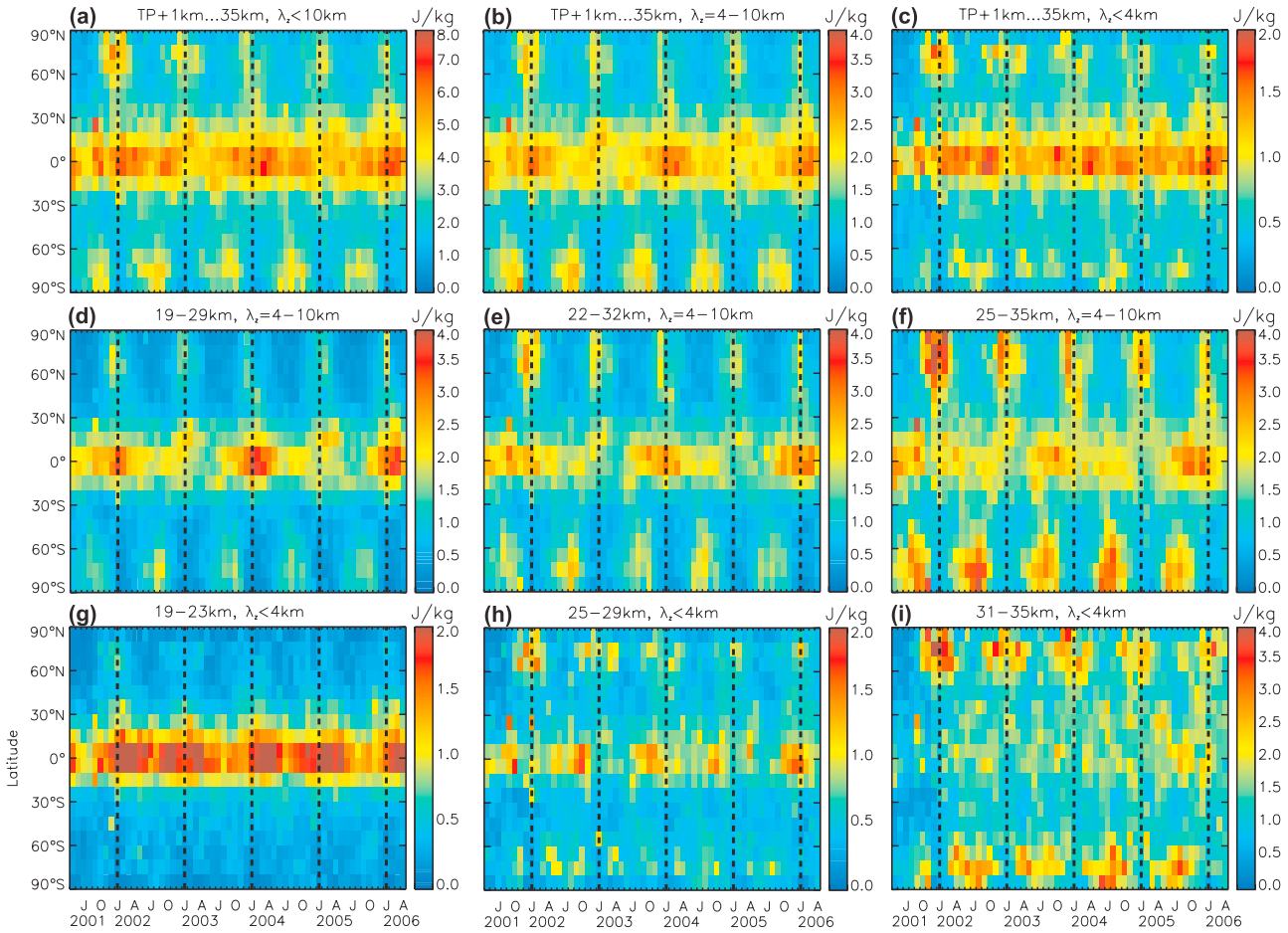

Figure 1. (a–c) E_{PC} distribution, averaged between 1 km above the TP and 35 km, for different bandpass cut-offs. (d–i) The same, for representative vertical columns consistent with the band-pass upper cutoffs selected: 10 and 4 km respectively.

We made several attempts to observe the sensitivity of choosing different starting altitudes above the TP and the corresponding effect is negligible (not shown), only slightly seen in the tropics. For example, In Figure 1b, choosing 1 or 2 km above the TP as starting altitude, the minimum/maximum E_{PC} values found are 0.4/3.3 J/kg and 0.3/3.1 J/kg, respectively. The starting point for the integration is 1 km above the last lapse rate TP (LRT), whereas in the tropics (30°N–30°S) we took the cold-point TP (CPT) if the CPT is higher than the last LRT, which happens sometimes in the tropics. So we took the last TP for each individual temperature profile [*Schmidt et al.*, 2006]. To get some insight into the vertical stratospheric stratification of these features, we apply vertical columns consistent with the band-pass upper cutoffs selected: 10 and 4 km respectively. In Figures 1d–1f, for long λ_z, C is 19–29 km, 22–32 km and 25–35 km, respectively. Figure 1d shows E_{PC} maximum values near 4 J/kg, with interannual equatorial and annual extratropical structures of enhanced WA. The tropical/extratropical signatures decrease/increase with increasing altitude. We are not able to state whether local or non local wave sources control the WA distribution at extratropical latitudes. A clear backwards monthly shift of the intense interannual equatorial maximum takes place. For short λ_z (Figures 1g–1i)), C is 19–23 km, 25–29 km and 31–35 km, respectively. An equatorial annual enhanced WA is only observed within 18–23 km between ±20° (Figure 1g) and to a lesser extent, within 25–29 km. There is a weakening of this periodic behavior around the Equator and a progressive enhancement of extratropical high latitude WA with increasing z (Figures 1h–1i). At 31–35 km maximum E_{PC} values are found only at high latitudes. In Figure 2, another approach to these features is presented, now showing E_P versus z. E_P, neglecting the factor g^2/N^2, is equivalent to the relative T variance. This last parameter was preferred by some authors [see, e.g., *Randel and Wu*, 2005] to present WA results. E_P has a "local" character, in the sense that it is not a measure of mean wave potential energy, averaged over a vertical interval, as shown in Figure 1. Its advantage is that the vertical resolution is retained. In Figure 2, the separation between long and short vertical wavelengths is performed again. The WA variability observed in Figure 1 led us to average E_P over 3 latitude bands: 1) 10°S–10°N, 2) 40°S–60°S and 3) 40°N–60°N, respectively. For long vertical wavelengths and 10°S–10°N, in Figure 2a, the period considered allows to identify a clear progression of WA enhancements, tightly following the QBO period and aligned with the z-time variability of background mean zonal winds. Wind data obtained from the global radiosonde network were zonally averaged here.

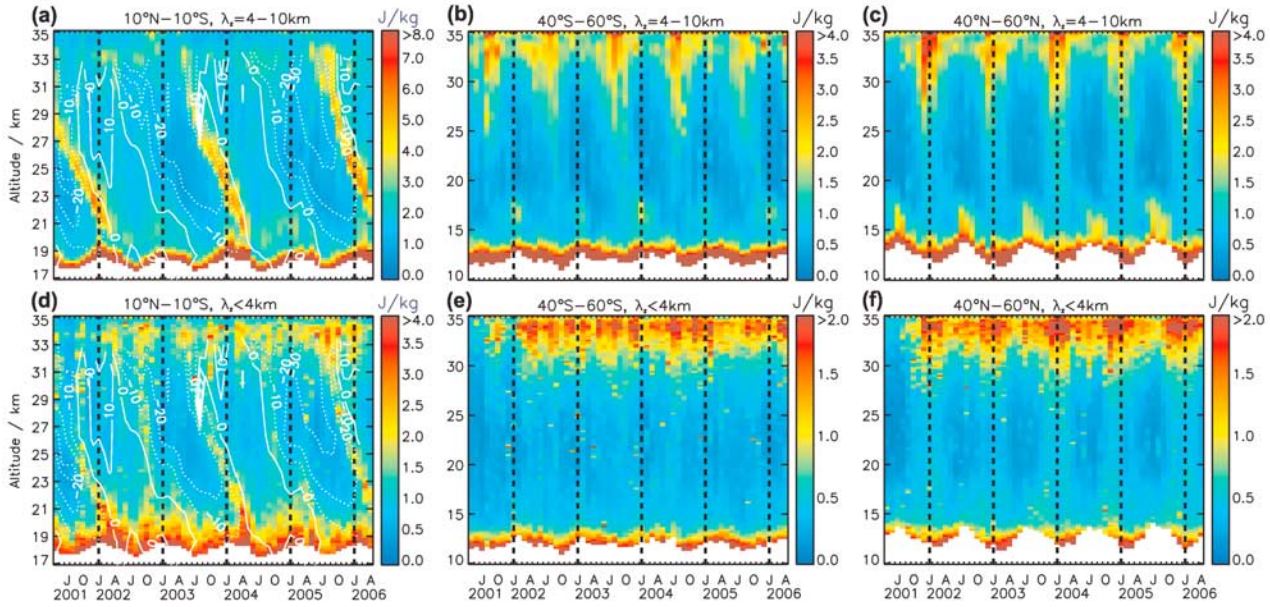

Figure 2. Height-month variation of E_P near to the Equator and within two latitude bands in both hemispheres, separated into (a–c) long and (d–f) short "apparent" vertical wavelengths.

[6] Three vertical regions with enhanced WA were identified here: 1) just below the zonal wind zero contours corresponding to westerly shears [see, e.g., *Randel and Wu*, 2005, and references therein], with E_P values near 7 J/kg, 2) immediately above the TP at equatorial latitudes, following its annual height oscillation [*Schmidt et al.*, 2005], and 3) above 30 km height. Significant decreases of WA are seen where the zonal wind is minimum. QBO is a wavelike structure of vertical wavelength about 20 km. *Schmidt et al.* [2005] have shown that QBO can be observed in GPS-RO data and has T amplitude of 4 K. In our analysis, to verify that we only retained gravity, inertio-gravity and planetary WA contributions, thus excluding the QBO T oscillation itself, we detrended the T data by zonal means. This procedure should remove the QBO. In doing so, Figure 2a remained unchanged, thus providing a proof that the described patterns are sound. This was expected, as we are considering and isolating only deviations from each individual profile. Figure 2b shows, for 40–60°S, in addition to the high E_P values near to the TP, the height distribution of enhanced WA during the Southern Spring Equinox, anticipated in Figures 1b and 1f. This enhanced WA, associated during 2002 to the stratospheric warming observed during that year [see, e.g., *Venkat Ratnam et al.*, 2004] appears here as a systematic annual stratospheric feature. Its intensity increases with altitude, from 25 to 35 km. IGWs generated by geostrophic adjustment during the maximum of the southern polar vortex (polar night jet) between late August and mid- September, could constitute a main source of this enhancement. A last sector of enhanced WA is annually observed from December to February, between 15 and 20 km height. In NH (Figure 2c), similar features to SH are seen in three sectors: 1) near the TP, 2) during winter between 25 and 35 km height and 3) from July to September between 15 and 20 km height. These last appear more intense than those mentioned in Figure 2b, at the same altitudes. For short vertical wavelengths, the WA distribution in Figure 2d is similar to Figure 2a, but reaching only half the maximum E_P values. Finally, in Figures 2e and 2f we only remark a persistent WA near to the TP and from 25 to 35 km (mainly in winter NH).

4. Concluding Remarks

[7] We presented the first results of a 5-year data analysis of stratospheric WA. The data set corresponds to GPS-RO T profiles, globally retrieved from the CHAMP satellite from May 2001 to April 2006. We considered only the contribution of gravity, inertio-gravity and planetary waves, with apparent λ_z below 10 km, excluding expected T variations due to the wavelike QBO behaviour. We underlined the difference between the two parameters used to describe the potential and mean potential energy distribution. Possible observational limitations and distortions expected from this wave analysis were pointed out. A sensitivity study suggested to choose 1 km above the tropopause, as a realistic starting altitude to calculate E_{PC}, avoiding possible artifacts caused during the filtering process. From these long-term observations, we confirmed previously reported features of WA distribution as a function of latitude, z and time, as well as other features not reported before. Stronger (weaker) WA is observed associated to apparent vertical wavelengths longer (shorter) than 4 km. The tropical/extratropical signatures decrease/increase with increasing altitude. At equatorial latitudes, WA annual enhancements, related to QBO, are observed just below zonal wind zero contours corresponding to westerly shears. A significant decrease of WA is seen where the zonal wind is minimum. Both at equatorial and middle latitudes, an increased WA appears close above the TP, following its annual height oscillation and above 30 km height. At higher latitudes, an annual variation of WA is observed during the 5 years analyzed, exhibiting stronger enhancements in winter SH respect to NH. In SH, they take place during late winter and early

spring. This enhanced WA, associated during 2002 to the stratospheric warming observed in that year, seems to be a systematic annual stratospheric characteristic. A significant contribution to this WA increase could be attributed to inertio-gravity waves generated by geostrophic adjustment, during the southern polar vortex (polar night jet) maximum between late August and mid- September. This jet may diffract typical inertio-gravity waves towards longer λ_z values, making it visible through the 4–10 km band-pass window.

[8] **Acknowledgments.** We thank all members of the CHAMP team, led by M. Rothacher, for their excellent work, which is the basis for our investigations. Helpful comments from S. Heise and G. Beyerle are acknowledged. We thank K. Schöllhammer for making available global radiosonde data via FU Berlin. The analysis of the RO measurements from CHAMP is partly funded by the German Research Foundation (DFG), grant WI2634/2-1/503976 (within CAWSES). The main authors thank GFZ Potsdam for the funding of a long-term research stay, during which the main work for the publication was done. One of the authors (A. de la Torre) is a member of CONICET under grant PIP 5932, and wishes to thank GeoForschungsZentrum Potsdam, for research conditions and the kind hospitality provided.

References

Alexander, M. J. (1998), Interpretations of observed climatological patterns in stratospheric gravity wave variance, *J. Geophys. Res.*, *103*, 8627–8640.

de la Torre, A., and P. Alexander (1995), The interpretation of wavelengths and periods as measured from atmospheric balloons, *J. Appl. Meteorol.*, *34*, 2747–2754.

de la Torre, A., and P. Alexander (2005), Gravity waves above Andes detected from GPS radio occultation temperature profiles: Mountain forcing?, *Geophys. Res. Lett.*, *32*, L17815, doi:10.1029/2005GL022959.

de la Torre, A., et al. (2004), A global distribution of the stratospheric gravity wave activity from GPS occultation profiles with SAC-C and CHAMP, *J. Meteorol. Soc. Jpn.*, *82*, 407–417.

Fritts, D. C., and M. J. Alexander (2003), Gravity wave dynamics and effects in the middle atmosphere, *Rev. Geophys.*, *41*(1), 1003, doi:10.1029/2001RG000106.

Gill, A. E. (1982), *Atmosphere-Ocean Dynamics*, Elsevier, New York.

Randel, W. J., and F. Wu (2005), Kelvin wave variability near the equatorial tropopause observed in GPS radio occultation measurements, *J. Geophys. Res.*, *110*, D03102, doi:10.1029/2004JD005006.

Scavuzzo, C. M., M. A. Lamfri, H. Teitelbaum, and F. Lott (1998), A study of the low-frequency inertio-gravity waves observed during the Pyrénés Experiment, *J. Geophys. Res.*, *103*(D2), 1747–1758.

Schmidt, T., et al. (2005), GPS radio occultaion with CHAMP and SAC-C: Global monitoring of thermal tropopause parameters, *Atmos. Chem. Phys.*, *5*, 1473–1488.

Schmidt, T., G. Beyerle, S. Heise, J. Wickert, and M. Rothacher (2006), A climatology of multiple tropopauses derived from GPS radio occultations with CHAMP and SAC-C, *Geophys. Res. Lett.*, *33*, L04808, doi:10.1029/2005GL024600.

Schönwiese, C. D. (2000), *Praktische Statistik für Meteorologen und Geowissenschaftler*, 296 pp., Gebrüder Borntraeger, Berlin.

Tsuda, T., M. Nishida, C. Rocken, and R. H. Ware (2000), A global morphology of gravity wave activity in the stratosphere revealed by the GPS occultation data (GPS/MET), *J. Geophys. Res.*, *105*(D6), 7257–7274.

Venkat Ratnam, M., G. Tetzlaff, and C. Jacobi (2004), Global and seasonal variations of stratospheric gravity wave activity deduced from the CHAMP/GPS satellite, *J. Atmos. Sci.*, *61*, 1610–1620.

Vincent, R. A., and M. J. Alexander (2000), Gravity waves in the tropical lower stratosphere: An observational study of seasonal and interannual variability, *J. Geophys. Res.*, *105*, 17,971–17,982.

Wickert, J., et al. (2005), GPS radio occultation with CHAMP and GRACE: A first look at a new and promising satellite configuration for global atmospheric sounding, *Ann. Geophys.*, *23*, 653–658.

Wu, D. L., et al. (2006), Remote sounding of atmospheric gravity waves with satellite limb and nadir techniques, *Adv. Space Res.*, in press.

Yoshiki, M., and K. Sato (2000), A statistical study of gravity waves in the polar regions based on operational radiosonde data, *J. Geophys. Res.*, *105*, 17,995–18,012.

A. de la Torre, Departamento de Fisica, Facultad de Ciencias Exactas y Naturales, Universidad de Buenos Aires, Ciudad Universitaria, 1428 Buenos Aires, Argentina. (delatorr@df.uba.ar)

T. Schmidt and J. Wickert, Geodesy and Remote Sensing, GeoForschungsZentrum Potsdam, Telegrafenberg A17, Potsdam, D-14473, Germany. (tschmidt@gfz-potsdam.de; jens.wickert@gfz-potsdam.de)